

MODELLING THE FRAME ERROR RATE FOR ITERATIVE DEMAPPING AND DECODING TECHNIQUES OVER QUASI-STATIC FADING CHANNELS

W. R. Carson and I. J. Wassell
Computer Laboratory
University of Cambridge
United Kingdom

M. R. D. Rodrigues
Instituto de Telecomunicações
Department of Computer Science
University of Porto, Portugal

Abstract — In this paper, we present and validate an analytical model for the frame error rate (FER) performance of iterative demapping and decoding techniques over quasi-static fading channels both with and without antenna diversity. In particular, the model characterises the FER performance in terms of four parameters only; the convergence threshold, the number of receive antennas, the number of transmit antennas, and the ratio of the energy per bit to the noise spectral density (E_b/N_0). We also discuss some complications arising in the estimation of the convergence threshold from extrinsic information transfer (EXIT) charts, for various mapping schemes, different coding schemes and decoding algorithms. Results demonstrate that system characteristics over quasi-static fading channels are accurately captured by the model.

I. INTRODUCTION

The turbo principle was conceived over a decade ago by Berrou *et al.* [1]. The authors proposed an encoder consisting of the parallel concatenation of two recursive systematic convolutional (RSC) encoders separated by a pseudo-random interleaver, and the corresponding turbo decoder consisting of two component soft-input soft-output decoders that exchange soft information in an iterative manner. Turbo codes show an impressive performance, closely approaching the Shannon limit.

Turbo or iterative techniques have since been proposed for a large number of communication scenarios including multi-user processing [2], space-time processing [3] and the processing of bit interleaved coded modulation (BICM) [4]. They have been shown to exhibit excellent performance over the additive white Gaussian noise (AWGN) channel [1]. In particular, it has been demonstrated that different system parameters, e.g., the interleaver size and the constituent RSC codes in the case of turbo codes, can dramatically affect the performance of iterative techniques over AWGN channels. Moreover, it has been also shown that they perform very well over fast fading channels [5], however they perform poorly over slow fading channels [6]. Essentially, over rapidly fading channels interleaving can be used as a means to create diversity by spreading the transmit symbols over multiple independently fading blocks in order to enhance performance. However, over slow fading channels interleaving cannot be used as a means to create diversity owing to delay and latency considerations. This situation compromises performance because occasional deep fades will affect the entire transmit frame causing severe error propagation in the iterative receiver [7].

The quasi-static fading situation is extremely important because it models various practical scenarios characterized by extremely low time and frequency diversity, e.g., fixed wireless access (FWA) channels. Bouzekri *et al.* [8] as well as Ro-

drigues *et al.* [9] have studied the effect of quasi-static fading channels on the performance of turbo codes. In particular, Rodrigues *et al.* presented an analytical framework based on a simple model described by El Gamal and Hammons [7]. Key to the derivation of the FER framework is that there are zero or negligible decoding errors above a particular E_b/N_0 value, termed the convergence threshold. However in an iterative demapping and decoding scenario [10] the use of a mapper as an inner encoder enables two other scenarios to arise: in the first instance a convergence threshold does not exist and in the second the decoding errors above the convergence threshold are non-negligible.

Consequently, this paper follows this line of work by investigating in detail the robustness of the framework in [9] in modelling the performance of the iterative demapping and decoding schemes proposed by ten Brink over quasi-static fading channels both with and without antenna diversity. Section II introduces the system model. Section III presents the analytical framework for modelling the performance of iterative schemes over quasi-static fading channels. Section IV provides a range of simulation results. In particular, it considers the effect on the system performance of various mapping schemes, different coding schemes, different decoding algorithms as well as space diversity. This section also illustrates how to estimate the key model parameters using EXIT charts, specifically emphasizing the problems that arise in the estimation process when using sub-optimal demapping and decoding. Finally, the main conclusions of this work are summarized in Section V.

II. SYSTEM MODEL

Fig.1 depicts the communications system model. We consider both single antenna systems ($N_T = N_R = 1$) often known as single-input single-output (SISO), which do not exploit space diversity, as well as multiple-input multiple-output (MIMO) antenna systems ($N_T, N_R > 1$), which do exploit space diversity. The transmitter consists of four main stages: the encoder, the interleaver, the mapper and the space-time processor (see Fig.1). Initially, the information bits are convolutionally encoded, at rate R_c , and these coded bits are then pseudo-randomly interleaved. Finally, groups of $\log_2 M$ interleaved coded bits are mapped to a complex symbol from a unit power M -ary quadrature amplitude modulation (QAM) constellation.

In single transmit antenna systems ($N_T = 1$), the space-time processing block does not further process the mapped symbols; instead, the mapped symbols are directly sent to the transmission block. However, in multiple transmit antenna systems ($N_T > 1$), the space-time processing block will further pro-

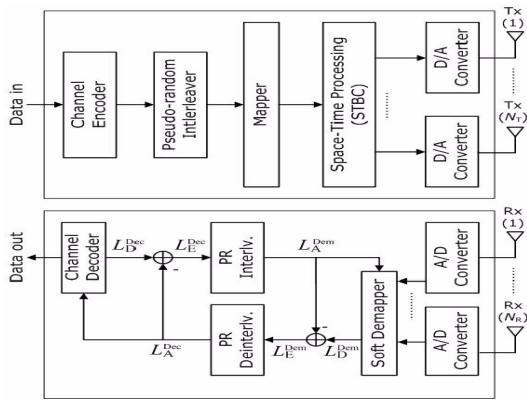


Figure 1: Communications system model.

cess the mapped symbols. In particular, the space-time processor generates a space-time block code (STBC) according to the generator matrices \mathbf{G}_2 , \mathbf{G}_3 or \mathbf{G}_4 given by [9]. Essentially, a total of $K \times N_T$ symbols obtained from the original K' modulation symbols are transmitted during K time slots by N_T transmit antennas. Note that \mathbf{G}_2 , \mathbf{G}_3 or \mathbf{G}_4 are appropriate for two, three and four transmit antennas, respectively, and for an arbitrary number of receive antennas. The ratio $R_s = \frac{K'}{K}$ denotes the rate of the STBC. Note also that \mathbf{G}_2 is rate $R_s = 1$, whereas \mathbf{G}_3 and \mathbf{G}_4 are rate $R_s = \frac{1}{2}$.

The signal is distorted by a frequency-flat quasi-static fading channel as well as AWGN. Therefore, the relationship between the complex receive symbols and the complex transmit symbols associated with a specific STBC frame may be written:

$$\mathbf{r} = \mathbf{h}\mathbf{s} + \mathbf{n}. \quad (1)$$

Here, \mathbf{r} denotes the N_R by K matrix whose element $r_j(k)$ denotes the complex receive symbol at time slot k and receive antenna j ; \mathbf{s} denotes the N_T by K matrix whose element $s_i(k)$ denotes the complex transmit symbol at time slot k and transmit antenna i ; \mathbf{h} denotes the N_R by N_T matrix of channel gains whose element $h_{j,i}$ denotes the channel gain from transmit antenna i to receive antenna j (note that $h_{j,i}$ is independent of time slot k); and \mathbf{n} denotes the N_R by K matrix whose element $n_j(k)$ denotes the noise random variable at time slot k and receive antenna j . The channel gains are uncorrelated circularly symmetric complex Gaussian with mean zero and variance $\frac{1}{2}$ per dimension. The noise random variables are uncorrelated circularly symmetric complex Gaussian with mean zero and variance $\frac{1}{2 \cdot \text{SNR}_{norm}} = \frac{N_T}{2 \cdot \text{SNR}}$ per dimension, where SNR denotes the average signal-to-noise ratio per receive antenna.

The receiver consists mainly of two stages: (i) the soft demapper and (ii) the soft-in soft-out decoder, which are separated by pseudo-random interleavers and de-interleavers. These two stages exchange soft information in an iterative manner (see Fig.1). Specifically, the soft demapper takes as *a priori* information $L_A^{Dem}(b_m(k))$ on the code bits which is an interleaved version of the extrinsic information $L_E^{Dec}(b_m(k))$ on the code bits produced by the soft-input soft-output decoder, where $b_m(k)$ is the m th bit conveyed by the k th mapped symbol. Then, it computes the *a posteriori* information $L_D^{Dem}(b_m(k)|\mathbf{r})$

of the code bits produced by the soft-input soft-output decoder - a log-likelihood ratio (LLR) - given by:

$$\begin{aligned} L_D^{Dem}(b_m(k)|\mathbf{r}) &= \ln \frac{\Pr(b_m(k)=1|\mathbf{r})}{\Pr(b_m(k)=0|\mathbf{r})} = \ln \frac{\sum_{(\mathbf{s} \in \mathbf{s}^+)} p(\mathbf{r}|\mathbf{s}) \Pr(\mathbf{s})}{\sum_{(\mathbf{s} \in \mathbf{s}^-)} p(\mathbf{r}|\mathbf{s}) \Pr(\mathbf{s})} \\ &= \ln \frac{\Pr(b_m(k)=1)}{\Pr(b_m(k)=0)} + \ln \frac{\sum_{(\mathbf{s} \in \mathbf{s}^+)} p(\mathbf{r}|\mathbf{s}) \prod_{\substack{m'=1 \\ m' \neq m}}^{K'} \prod_{\substack{k'=1 \\ k' \neq k}}^{K'} \Pr(b_{m'}(k'))}{\sum_{(\mathbf{s} \in \mathbf{s}^-)} p(\mathbf{r}|\mathbf{s}) \prod_{\substack{m'=1 \\ m' \neq m}}^{K'} \prod_{\substack{k'=1 \\ k' \neq k}}^{K'} \Pr(b_{m'}(k'))} \end{aligned} \quad (2)$$

where \mathbf{s}^+ is the set of matrices of transmit symbols \mathbf{s} such that $b_m(k) = 1$ (i.e., $\mathbf{s}^+ = \{\mathbf{s}: b_m(k) = 1\}$), \mathbf{s}^- is the set of matrices of transmit symbols \mathbf{s} such that $b_m(k) = 0$ (i.e. $\mathbf{s}^- = \{\mathbf{s}: b_m(k) = 0\}$). The soft demapper is able to simplify this calculation by using the Jacobian logarithm [11], which we will refer to as *max** demapping. Furthermore this can again be simplified by using the *max.* approximation to the Jacobian, and we shall refer to this as *max.* demapping. Finally, the soft demapper passes the extrinsic information $L_E^{Dem}(b_m(k)) = L_D^{Dem}(b_m(k)|\mathbf{r}) - L_A^{Dem}(b_m(k))$ on the code bits to the subsequent stage - the soft-in soft-out decoder.

Likewise, the soft-input soft-output channel decoder takes as *a-priori* information a de-interleaved version of the extrinsic information produced by the soft demapper. Then, it computes the *a-posteriori* information, using a soft-input soft-output decoding algorithm, e.g., the log-MAP algorithm or the SOVA algorithm [11]. Finally, the soft-input soft-output decoder passes the extrinsic information back to the the soft demapper.

III. ANALYTICAL FRAMEWORK

We now consider an analytic framework to assess the frame error rate (FER) of the iterative demapping and decoding system over quasi-static fading channels with and without antenna diversity. In particular, we will characterize the FER in terms of specific system parameters, namely, the number of transmit and receive antennas, the energy per bit to the noise power spectral density, γ_b , and the convergence threshold γ_{th} . This analytic framework is based on a similar framework in [9] applicable for turbo codes, which in turn builds upon a simple model proposed by El Gamal and Hammons [7].

Assume transmission over an AWGN channel. We then assume that for an iterative system when $\gamma_b \leq \gamma_{th}$ the decoder frame error rate is bounded away from zero, whereas when $\gamma_b > \gamma_{th}$ the decoder frame error rate approaches zero as the number of decoding iterations increases. Consequently, it is very simple to estimate the FER performance since the quasi-static fading channel corresponds to a faded AWGN channel. The instantaneous $\gamma_b = \frac{1}{R_c} \frac{1}{R_s} \sum_{i,j} |h_{j,i}|^2 \text{SNR}_{norm}$ follows a chi-squared distribution with $2N_T N_R$ degrees of freedom [9]. Consequently the frame error rate is given by, where $\bar{\gamma}_b$ is the

average value of γ_b .

$$\text{FER} = 1 - e^{\left(\frac{-\gamma_{th}}{\bar{\gamma}_b/N_T N_R}\right)} \left\{ 1 + \sum_{k=0}^{N_T N_R - 1} \frac{1}{k!} \left(\frac{\gamma_{th}}{\bar{\gamma}_b/N_T N_R}\right)^k \right\}. \quad (3)$$

We observe that the final term in (3) is the power series expansion of $e^{\left(\frac{\gamma_{th}}{\bar{\gamma}_b/N_T N_R}\right)}$ truncated after $N_T N_R$ terms. Note that $a_n = 0$ for all n in the series expansion of $e^{-x} e^x$ in (4).

$$\begin{aligned} e^{-x} e^x &= (1 - x + \frac{x^2}{2!} - \frac{x^3}{3!} + \dots)(1 + x + \frac{x^2}{2!} + \frac{x^3}{3!} + \dots) \\ &= 1 + a_1 x + a_2 x^2 + a_3 x^3 + \dots \end{aligned} \quad (4)$$

We note that the terms x^n cannot affect the coefficients of lower order terms, therefore in the truncated series $a_n = 0$ for $0 < n < N_T N_R$. Furthermore, the contribution that the truncated terms would have given to a_n for $n \geq N_T N_R$ must exactly balance the contribution due to the untruncated terms, e.g., only the truncated $x^{N_T N_R}$ term would contribute to $a_{N_T N_R}$, therefore $a_{N_T N_R} = \frac{-1}{(N_T N_R)!}$. The general term is:

$$a_n = \sum_{k=0}^{n - N_T N_R} \frac{(-1)^{k+1}}{(n-k)! k!}, \text{ for } n \geq N_T N_R.$$

We consider the performance of the model for E_b/N_0 values above the convergence threshold; the performance will be dominated by the polynomial term of order $N_T N_R$, since $a_n = 0$ for $0 < n < N_T N_R$. Consequently, we can further simplify the FER expressions for the high $\bar{\gamma}_b$ regime in decibels:

$$\text{FER}_{dB} = \frac{N_T N_R}{10} (\gamma_{th} - \bar{\gamma}_b) + \log_{10} \left[\frac{(N_T N_R)^{N_T N_R}}{(N_T N_R)!} \right]. \quad (5)$$

These expressions tell us that the gradient of the FER plots depends only on the number of transmit and receive antennas.

IV. SIMULATION RESULTS

This section investigates the robustness of the analytical framework in modelling the performance of an iterative demapping and decoding system over frequency-flat quasi-static fading channels both with and without antenna diversity. We consider various mapping schemes including 16-QAM with Gray, anti-Gray and Boronka mappings (see [10] for details), with either *max** or *max* demapping. We also consider various coding schemes, rate 1/2 RSC codes with memory two (octal generator polynomial (1, 5/7)) and four (octal generator polynomial (1, 21/37)) with either log-MAP or SOVA decoding. We denote the combination of *max** demapping and log-MAP decoding by *max** log-MAP decoding, with extensions to *max* demapping and SOVA decoding. We use EXIT charts [12] to estimate the convergence threshold γ_{th} for the various system configurations, since it is not possible to perform such estimation with analytic techniques. In particular, we will determine both the transfer characteristics and the decoding trajectories for a frame length of 10^6 bits. In contrast, we will determine the FER performance for a frame length of 2048 bits, averaged over 10^4 realisations per E_b/N_0 value. Note that even though the convergence threshold is only an appropriate measure for very long frames, e.g., 10^6 bits, the analytical framework still produces very accurate FER results for shorter frames.

A. EXIT charts: Estimating γ_{th}

The convergence threshold is defined as the lowest possible E_b/N_0 value that allows the decoding trajectory to traverse the entire EXIT chart. It has been observed for turbo codes that γ_{th} is also given by the E_b/N_0 value that causes the characteristic curves of the constituent codes to just touch and hence pinch-off any possible trajectory from traversing the chart [12].

Decoding algorithm	RSC Encoder	Demapper	γ_{th} Estimate (dB)	
			anti-Gray	Boronka
MAP	(1,5/7)	<i>max*</i>	4.7	3.7
		<i>max</i>	5.2 (4.8)	4.0 (3.8)
	(1,21/37)	<i>max*</i>	5.3	4.2
		<i>max</i>	5.7 (5.4)	4.6 (4.3)
SOVA	(1,5/7)	<i>max*</i>	5.7 (3.7)	4.7 (2.9)
		<i>max</i>	5.8 (3.8)	4.9 (3.1)
	(1,21/37)	<i>max*</i>	6.3 (4.1)	5.3 (3.4)
		<i>max</i>	6.4 (4.2)	5.4 (3.5)

Table 1: Convergence thresholds for anti-Gray and Boronka, with RSC codes (1,5/7) and (1,21/37). Estimates using characteristic curves are in brackets.

1) *Max** log MAP decoding

We observe that the trajectory plot follows the EXIT chart characteristic curves and hence both predict the same convergence threshold, Fig. 2. Generally, we would choose to calculate γ_{th} using the characteristic curves, rather than the decoding trajectory, since these are less computationally expensive to simulate. Once we have constructed the EXIT chart, we are able to predict certain qualitative aspects of the FER performance plots. The value of γ_{th} is affected by the initial part of the curves on the EXIT chart and initially, the (1,21/37) curve lies above the (1,5/7) curve. This implies that for both anti-Gray and Boronka mappings the lower memory code would have a lower γ_{th} . It is important to note that schemes such as Gray mapping will not have a convergence threshold due to the shallow gradient of the demapping characteristic curves and therefore, FER performance is dominated by the final portion of the curves on EXIT charts; where the (1,21/37) curve now lies below the (1,5/7) curve. This implies that for Gray mapping, the (1,21/37) code has the better FER performance curve.

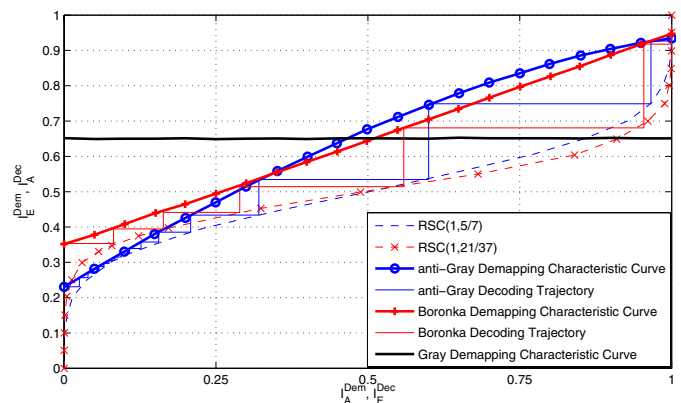


Figure 2: EXIT chart characteristic curves and decoding trajectories. All curves were recorded for an $E_b/N_0 = 4.7$ dB with *max** log-MAP decoding.

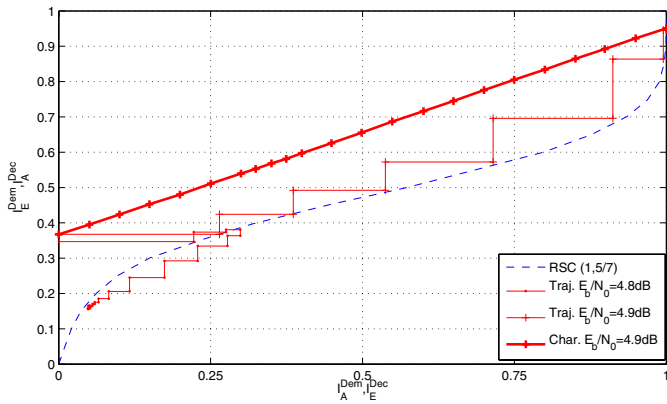


Figure 3: EXIT chart characteristic curves for Boronka mapping and RSC encoding with generator polynomial (1,5/7), and *max.* SOVA decoding.

2) Demapping with *max.* and SOVA decoding

Unfortunately, when we replace either *max** with *max.* demapping or log-MAP by SOVA decoding or both, the characteristic curves of the EXIT chart and the decoding trajectories no longer match, Fig. 3, and therefore they generate two different values for γ_{th} , Table 1. The convergence threshold is increased by about 0.3dB by using *max.* demapping and 2.0dB by using SOVA decoding. It is also interesting to note that due to the deforming of the decoder curve with SOVA compared to the MAP algorithm, the characteristic curves actually predict a lower γ_{th} with SOVA than with MAP, Table 1.

We further observe that after the fourth iteration of the $E_b/N_0 = 4.8$ dB decoding trajectory the mutual information actually begins to decrease. This is particularly interesting and unexpected because it implies that at the fourth iteration an increase in the I_A^{Dem} actually decreases the I_E^{Dem} . The SOVA decoding is known to overestimate the extrinsic information [13] and we believe that this overconfidence causes the decrease in I_E^{Dem} at the demapper output after the fourth iteration.

3) EXIT Chart Assumptions

Characteristic curves are simulated under the assumption that the input *a-priori* information is drawn from a single Gaussian distribution. Fàbregas and Grant [14] investigated an iterative demapping and decoding scheme where the decoding trajectories did not follow the characteristic curves and reasoned that this was due to the non-Gaussian *a-priori* distribution.

We have already seen that when we use *max** log-MAP decoding, the decoding trajectory matches the characteristic curves, Fig. 2. In this scenario, we also observed that the *a-priori* information for our system is also non-Gaussian however the *a-priori* information is drawn from a single distribution, i.e. the average I_A^{Dem} per bit is the same.

We have also already seen that when we use *max* SOVA decoding, the decoding trajectory does not match the characteristic curves, Fig. 3. In this scenario, we also observed non-Gaussian *a-priori* information however the *a-priori* information is no longer drawn from a single distribution. Instead each of the bits in the 16-QAM symbol have different average I_A^{Dem} , i.e., the input *a-priori* information is drawn from four indepen-

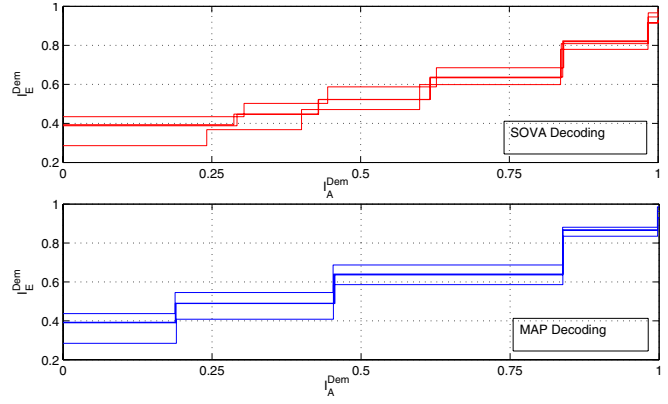


Figure 4: EXIT chart bit-wise decoding trajectories for Boronka mapping and RSC encoding with generator polynomial (1,5/7) for an $E_b/N_0 = 5$ dB decoded with *max.* SOVA and *max** log-MAP. Note that two of the four bit-wise decoding trajectories per EXIT chart overlap and are difficult to distinguish.

dent distributions, Fig. 4. We observed that the demapper is highly dependent on the weighting of mutual information over the bits in a symbol, therefore the four independent distributions will cause the decoding trajectory to deviate from the demapper characteristic curve. We get a similar effect of unevenly distributed average I_A^{Dem} if we implement *max.* instead of *max** demapping with log-MAP decoding.

B. FER Results

Once we have an accurate estimate of the convergence threshold we are able to assess the robustness of the model to different mapping schemes and coding schemes. Fig. 5 depicts the FER versus E_b/N_0 performance curves for *max** demapping and log-MAP decoding obtained both by analysis and simulation. We denote MIMO scenarios with shorthand notation, e.g., 4Tx4Rx means four transmit and four receive antennas.

The model predicts that any curves that have the same antenna diversity will have the same gradient for $\bar{\gamma}_b \gg \gamma_{th}$, see

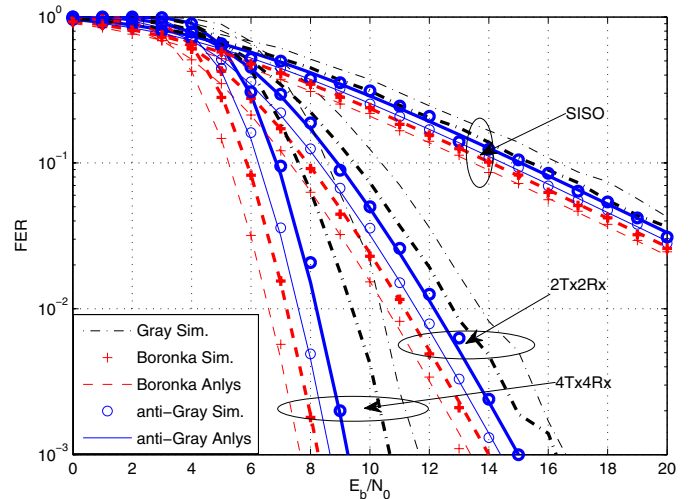


Figure 5: FER versus E_b/N_0 performance curves for an iterative system with *max** log-MAP decoding. The RSC code generator polynomials are (1,5/7) (thin lines and symbols) and (1,21/37) (bold lines and symbols).

(5), therefore in this region and for a fixed FER, the performance gain in dB of one scheme over another corresponds to the difference in dB between the convergence thresholds. We observe that for the anti-Gray and Boronka mappings, the analytical model is a good approximation to the simulated FER curves. Furthermore, since the gradient of the Gray mapping 4Tx4Rx curve differs from the others, we would be unable to model it accurately. We also observe that both anti-Gray and Boronka mappings outperform Gray mapping for systems both with and without antenna diversity.

Increasing the constraint length of the RSC encoder affects non-iterative and iterative mappings schemes differently; the FER performance for both anti-Gray and Boronka mappings is made worse whereas the FER performance improves for Gray mapping. We were able to predict this performance using both the analytical model and EXIT charts, by considering the shape of the characteristic curves at the beginning and end of the charts. In [10], we observed that for Gray mapping, longer memory codes have longer burst errors than shorter codes, however burst errors are more frequent for the shorter codes and this dominates performance, leading to longer codes outperforming them. We believe that for anti-Gray and Boronka mappings, the burst length dominates performance and leads to longer codes performing worse than to shorter codes.

We observe the robustness of the model to variations in the demapping and decoding algorithms, Fig. 6. For all decoding schemes that do not implement max^* log-MAP decoding, we implement the convergence threshold estimated from the decoding trajectory since these are always the true values. As we would expect, by implementing max^* SOVA decoding we decrease the computational complexity at the expense of FER performance. The max^* demapping approximation has a less profound effect in terms of γ_{th} estimation and reduced FER performance compared with SOVA. Again since this scenario is modeled well we are able to estimate the performance of the decoding algorithms at low FER as the difference in convergence thresholds, e.g. at a FER = 10^{-3} , max^* log-MAP decoding is $4.9 - 3.7 = 1.2$ dB better than max^* SOVA decoding.

We finally observe that we are able to accurately model the FER performance for a frame length of 2048 bits, even though γ_{th} was estimated using a much longer frame length, 10^6 bits.

V. CONCLUSIONS

In this paper we have investigated in detail the performance of an analytical model for iterative demapping and decoding techniques over quasi-static fading channels both with and without antenna diversity. In particular, we have considered the accuracy of such a model for BICM-ID and the effect on the accuracy of the model to variations of the system parameters, including different demapping strategies, different decoding algorithms, different mapping schemes and different coding schemes. Results demonstrated that the model can capture the FER performance when we are able to accurately estimate the convergence threshold. Difficulties in estimating the convergence threshold arising from the use of sub-optimal demapping and decoding are also discussed.

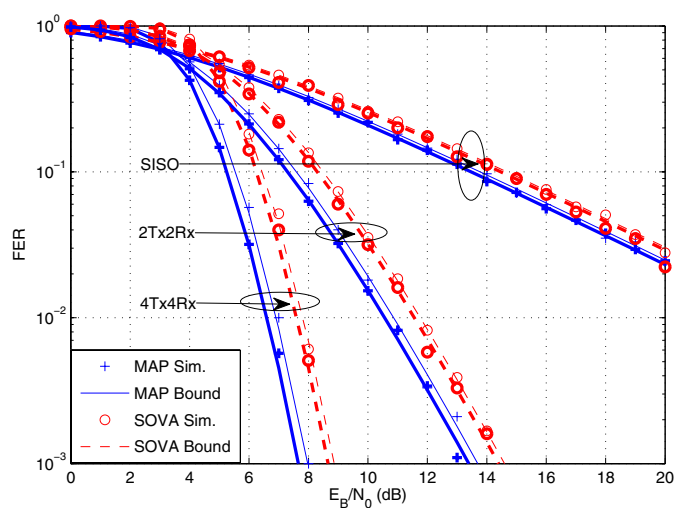


Figure 6: FER versus E_b/N_0 performance curves for an iterative system with Boronka mapping and RSC code generator polynomial (1,5/7), for demapping with max^* (bold lines and symbols) and with max^* (thin lines and symbols).

ACKNOWLEDGMENT

The authors would especially like to thank Dr. Ioannis Chatzigeorgiou for valuable discussions and comments.

REFERENCES

- [1] C. Berrou and A. Glavieux, "Near optimum error correcting coding and decoding: Turbo codes," in *IEEE Trans. Commun.*, Oct. 1996.
- [2] X. Wang and H. V. Poor, "Iterative (turbo) soft interference cancellation and decoding for coded CDMA," in *IEEE Trans. Commun.*, July 1999.
- [3] B. Lu and X. Wang, "Iterative receivers for multiuser space-time coding systems," in *IEEE J. Select. Areas Commun.*, Nov. 2000.
- [4] S. ten Brink, J. Speidel, and R. H. Yan, "Iterative demapping and decoding for multilevel modulation," in *Proc. IEEE Globecom '98*, July 1998.
- [5] E. K. Hall and S. G. Wilson, "Design and analysis of turbo codes on Rayleigh fading channels," in *IEEE J. Select. Areas Commun.*, Feb. 1998.
- [6] L. Lin, L. J. Cimini, and C. I. Chuang, "Comparison of convolutional and turbo codes for OFDM with antenna diversity in high-bit-rate wireless applications," in *IEEE Commun. Lett.*, Sept. 2000.
- [7] H. E. Gamal and J. A. R. Hammons, "Analyzing the turbo decoder using the Gaussian approximation," in *IEEE Trans. Commun.*, Feb. 2001.
- [8] H. Bouzekri and S. L. Miller, "An upper bound on turbo codes performance over quasi-static fading channels," in *IEEE Commun. Lett.*, July 2003.
- [9] M. R. D. Rodrigues, I. A. Chatzigeorgiou, I. J. Wassell, and R. A. Carrasco, "On the performance of turbo codes in quasi-static fading channels," in *Proc. IEEE ISIT '05*, Sept. 2005.
- [10] W. R. Carson, I. Chatzigeorgiou, M. R. D. Rodrigues, I. J. Wassell, and R. Carrasco, "On the performance of iterative demapping and decoding techniques over quasi-static fading channels," in *Proc. PIMRC 2007*, Sept. 2007.
- [11] J. P. Woodard and L. Hanzo, "Comparative study of turbo decoding techniques: An overview," in *IEEE Trans. Veh. Technol.*, Nov. 2000.
- [12] S. ten Brink, "Convergence behaviour of iteratively decoded parallel concatenated codes," in *IEEE Trans. Commun.*, Oct. 2001.
- [13] L. Papke, P. Robertson, and E. Vilebrun, "Improved decoding with the sova in a parallel concatenated (turbo-code) scheme," in *Proc. Int. Conf. Commun.*, July 1996.
- [14] A. Guillén i Fàbregas and A. Grant, "Capacity approaching codes for non-coherent orthogonal modulation," to appear in *IEEE Trans. Wireless Commun.*